A CONTRIBUTION TO THE PROBLEM OF STRATOSPHERIC DIFFUSION BY LARGE-SCALE MIXING[1, 2]

RICHARD J. REED and KENNETH E. GERMAN

University of Washington, Seattle, Wash.

ABSTRACT

The assumption is commonly made in stratospheric diffusion studies that the large-scale eddy flux of various properties obeys the Fickian law which requires that the flux in a coordinate direction is proportional to and in the direction of the gradient. Measurements of eddy fluxes of ozone and sensible heat reveal, however, that the law is violated in the lower stratosphere where the meridional fluxes are countergradient at most latitudes.

Use is made of the mixing length hypothesis to derive a more general expression for the large-scale eddy flux which is able to account for the phenomenon of countergradient flux. It is found that the critical parameter in determining whether the horizontal flux is in the gradient or countergradient direction is the ratio of the mean slope of the mixing path (or surface) to the mean slope of the isopleths of the property being considered.

A procedure is outlined for evaluating the coefficients needed to solve the derived diffusion equation. Although exact solutions to the equation can be obtained only by numerical methods, it is possible, by use of a number of simplifying assumptions, to achieve a crude analytical solution. Only the results of the analytical solution are presented here. These pertain to the tungsten-185 injected into the lower equatorial stratosphere during the Hardtack nuclear test series of 1958. Good correspondence is obtained between the gross features of the predicted and observed distributions two months following the time of injection.

1. INTRODUCTION

The testing of nuclear weapons in the atmosphere renewed and heightened interest in the problem of stratospheric transport and diffusion. Considerable practical importance now attaches to the question of how rapidly and by what mechanisms trace substances introduced into one region of the stratosphere spread to other regions and eventually enter the troposphere and reach the ground.

An early speculation concerning stratospheric mass transport is found in a paper of Wulf [22] in which he attempts to account for the excess of ozone beyond its photochemical equilibrium amount at high latitudes. Wulf visualized a meridional circulation in which air descended in the equatorial stratosphere, moved poleward in the region above the tropopause, and ascended in the polar stratosphere. Similarly, meridional circulations, but of different character, have been invoked by Brewer [1] and Dobson [3] to explain the water vapor and ozone distributions in the stratosphere.

Though objections have been raised from the start to the Brewer-Dobson model, on such grounds as difficulties it poses with the momentum budget, it nevertheless received wide acceptance until Feely and Spar [5] presented the results of the experiment in which tungsten-185 was injected into the lower equatorial stratosphere during the Hardtack test series of 1958. Contrary to the prediction of the Brewer-Dobson circulation scheme, the center of the tungsten cloud remained nearly at the latitude of injection (11° N.) during the subsequent two years that measurements were taken. However concentrations within the cloud decreased and the boundaries spread poleward in a manner which suggested that large-scale quasi-horizontal mixing was the dominant transport mechanism. If a meridional cellular motion of the type prescribed by Brewer and Dobson was present, its effects were clearly overshadowed by the action of the large-scale eddies.

Despite the indications of the tungsten-185 experiment it would be premature to conclude that meridional circulations are unimportant in determining the transport properties of the stratosphere. For the present it would seem advisable to consider both advective and turbulent motions in any full treatment of the transport problem and to direct efforts toward obtaining the best possible descriptions of the two mechanisms. In the present paper we will consider only the large-scale mixing problem with the objective of pointing out the inadequacy of previous formulations in describing the type of mixing process that occurs in the lower stratosphere and of proposing a new formulation which overcomes the noted deficiency. Moreover a procedure is outlined whereby the proposed formulation may be put to practical use in obtaining numerical solutions to the diffusion equation.

Though we have not yet carried out the suggested procedures for obtaining numerical solutions, we have succeeded in obtaining predictions of the tungsten-185 distribution by means of a highly simplified analytical solution. The success of the analytical method in repro-

[1] Contribution No. 104, Department of Atmospheric Sciences, University of Washington, Seattle, Wash.

[2] This research was supported by the National Science Foundation under grant GP-2282.

ducing the gross features of the observed distribution encourages the hope that worthwhile numerical solutions will soon be obtained.

2. DIFFUSION EQUATION FOR GLOBAL TRANSPORT

The subsequent arguments and analysis are based on a specialized form of the diffusion equation suitable for the study of the meridional transport of trace substances on a global scale. This equation is derived as follows.

Let $\chi=c/\rho$ represent the mixing ratio of a trace substance, c being the concentration of the substance and ρ the air density. Then, in the absence of sources and sinks, the equation of mass continuity for the substance may be written

$$\frac{\partial}{\partial t}(\rho\chi)=-\nabla\cdot(\rho\chi\mathbf{V}) \tag{1}$$

where $\mathbf{V}$ is the velocity. Averaging (1) with respect to time, t, and longitude λ and making use of the following definitions:

$$\bar{(\ )}\equiv\frac{1}{2\pi\tau}\int_0^{\tau}\int_0^{2\pi}(\ )d\lambda dt$$

the time-zonal average of ( ) over period τ, $(\ )'\equiv(\ )-\bar{(\ )}$ the deviation of ( ) from the time-zonal average, we obtain the diffusion equation in the form

$$\frac{\partial\bar{\chi}}{\partial t}=-\bar{\mathbf{V}}\cdot\nabla\bar{\chi}-\frac{1}{\rho a}\frac{\partial}{\partial\phi}\rho\overline{\chi'v'}-\frac{1}{\rho}\frac{\partial}{\partial z}\rho\overline{\chi'w'}+\frac{\tan\phi}{a}\overline{\chi'v'} \tag{2}$$

where a is the mean radius of the earth, ϕ is latitude, z is elevation, and v and w are the velocity components northward and upward. In deriving (2) the common assumption has been made that the fluctuations of density may be neglected compared with the fluctuations of χ and of the velocity components. Moreover terms which arise in the spherical coordinate system because of the divergence of the vertical coordinate have been neglected. It should be noted that a more sophisticated treatment might distinguish between transient eddies and standing eddies, but the complications introduced by such a separation would probably detract from our main arguments without offering any obvious advantages. In later sections where use is made of published data on wind variations and eddy heat fluxes we have in all cases combined the statistics for the two types of eddy processes when they have been given separately.

Alternatively (2) may be written

$$\frac{\partial\bar{c}}{\partial t}=-\bar{\mathbf{V}}\cdot\nabla\bar{c}-\Gamma\bar{w}\bar{c}-\frac{\partial}{\partial y}\rho\overline{\chi'v'}-\frac{\partial}{\partial z}\rho\overline{\chi'w'}+\frac{\tan\phi}{a}\rho\overline{\chi'v'} \tag{3}$$

where y is distance northward and $\Gamma\equiv-\rho^{-1}\partial\rho/\partial z$.

3. THE PROBLEM

The first two terms on the right-hand side of (3) express the effect of mean or meridional motions in changing the concentration of the trace substance. The remaining terms represent the concentration changes arising from the turbulent or eddy fluxes whose y and z components, F_y and F_z, are

$$F_y=\rho\overline{\chi'v'} \tag{4}$$

$$F_z=\rho\overline{\chi'w'} \tag{5}$$

For the purpose of putting (4) or (5) in a mathematically tractable form it is customary to express the eddy fluxes as the products of coefficients of eddy diffusion and gradients of the mixing ratio. Thus the assumption is commonly made that the component fluxes obey the Fickian law so that

$$F_y=-\rho K_y\frac{\partial\bar{\chi}}{\partial y} \tag{6}$$

$$F_z=-\rho K_z\frac{\partial\bar{\chi}}{\partial z} \tag{7}$$

where K_y and K_z are (positive) eddy diffusion coefficients in the y and z directions. Among the authors who have employed this assumption in large-scale diffusion studies mention may be made of Machta and List [10], Friend and Feely [6], Prabhakara [18], and Sundström [20]. However it must be stated that by and large these authors have recognized that (6) and (7) are not the general expressions for the flux components.

The inadequacy of equation (6) in representing the horizontal flux in the lower stratosphere is evident from a consideration of measurements of eddy heat flux (White [21], Murakami [12], and Peng [17]) and ozone flux (Newell [14], Hering and Borden [8]). In the case of both quantities it is found that the eddy flux in the meridional direction is countergradient; that is, the flux is in the direction from low to high value of the quantity rather than in the reverse direction as required by (6).

The physical explanation of the (horizontal) countergradient heat flux has been given by Newell [13]. The crux of the argument is that in the lower stratosphere air parcels generally subside as they move northward from the cold tropical regions, following an inclined path that possesses a greater slope than the undisturbed isentropic surfaces. Similarly, southward-moving parcels ascend with an inclination greater than that of the undisturbed isentropes. The effect is illustrated in figure 1 (where for the present purpose χ is imagined to represent the potential temperature). It is apparent that if the displacements are isentropic or quasi-isentropic, the northward-moving parcel will be anomalously warm and the southward-moving parcel anomalously cold as they pass through a surface normal to the y-axis. Thus the net heat transport is northward despite the southward-directed gradient. Moreover heat flux can occur along the y-axis even in the absence of a gradient along the axis.

From the foregoing considerations it is apparent that equations (6) and (7) are unsuitable for describing the

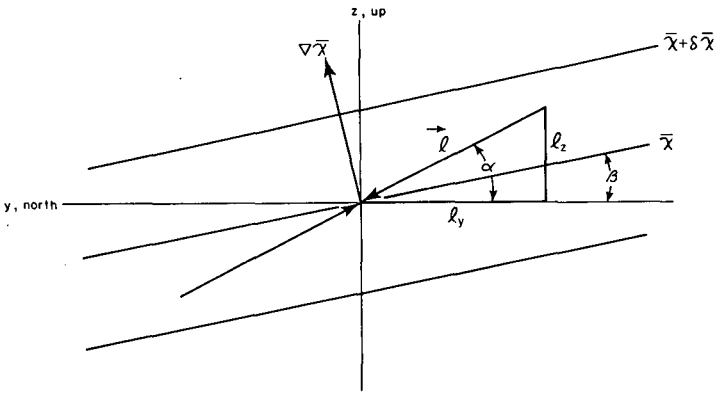

FIGURE 1.—Model for the eddy flux of a property by exchange along a sloping mixing path.

mixing process in the lower stratosphere. We will now employ the mixing length hypothesis to derive more satisfactory expressions.

4. REFORMULATION (I)

In the mixing length hypothesis it is assumed that an air parcel, starting as an average sample of its environment, moves a distance l (the mixing length) before it mixes suddenly and completely with the new environmental air and that during the displacement the property χ is conserved. If the mixing path is allowed to have any orientation in space, it is clear from figure 1 that the deviation of the conservative quantity χ from its mean value upon reaching the origin is given, to a first approximation, by

$$\chi' = -\mathbf{l}\cdot\nabla\bar{\chi} = -\left(l_y\frac{\partial\bar{\chi}}{\partial y}+l_z\frac{\partial\bar{\chi}}{\partial z}\right) \tag{8}$$

where $\mathbf{l}$ is the displacement vector and l_y and l_z are its horizontal and vertical components. Substitution of (8) in equations (4) and (5) yields for the component fluxes

$$F_y = -\rho\left(K_{yy}\frac{\partial\bar{\chi}}{\partial y}+K_{yz}\frac{\partial\bar{\chi}}{\partial z}\right) \tag{9}$$

$$F_z = -\rho\left(K_{zy}\frac{\partial\bar{\chi}}{\partial y}+K_{zz}\frac{\partial\bar{\chi}}{\partial z}\right) \tag{10}$$

where

$$K_{yy}\equiv\overline{l_y v'} \tag{11}$$

$$K_{yz}\equiv\overline{l_z v'} \tag{12}$$

$$K_{zy}\equiv\overline{l_y w'} \tag{13}$$

$$K_{zz}\equiv\overline{l_z w'} \tag{14}$$

It is apparent from (9) and (10) that in the general case two coefficients and both components of the gradient are needed to determine the flux in a coordinate direction. Only when the covariances of l_z and v' and l_y and w' are zero do these equations reduce to the commonly used forms (6) and (7). Such conditions on the covariances are equivalent to the assumption that the meridional and vertical wind components are uncorrelated during the exchange process, but this is contrary to the evidence (Molla and Loisel [11]).

5. REFORMULATION (II)

We will now derive alternative expressions for the eddy flux components. These will be useful later when we consider the practical problem of evaluating the diffusion coefficients. They will also be valuable in providing physical insight concerning the conditions governing whether the component fluxes are gradient or countergradient.

We first make the assumption that the velocity and displacement vectors have the same direction. Thus

$$\frac{w}{v}=\frac{l_z}{l_y} \tag{15}$$

This assumption will be permissible if the mixing length is small compared with the size of the eddies. Later measurements indicate that K_{yy} is of the order of 10^{10} cm.^{2} sec.$^{-1}$. Since v' is of the order of 10^3 cm. sec.$^{-1}$, the mixing length is only of the order of 100 km., a suitably small value. From (15) and the geometry of figure 1, it follows that

$$v' = V\cos\alpha = V\left(1-\frac{\alpha^2}{2}+\ldots\right)\simeq V \tag{16}$$

$$l_y = l\cos\alpha = l\left(1-\frac{\alpha^2}{2}+\ldots\right)\simeq l \tag{17}$$

$$w' = V\sin\alpha = V(\alpha+\ldots)\simeq V\alpha \tag{18}$$

$$l_z = l\sin\alpha = l(\alpha+\ldots)\simeq l\alpha \tag{19}$$

where V is the total wind speed and α is the angle that l makes with the horizontal. The approximations on the right may be justified by the fact that for large-scale motion α is of the order of 1:1000 at most. Since $\alpha\simeq\tan\alpha$ for small angles, we will hereafter refer to it as the slope of the mixing path (or surface). Substitution of (16)–(19) in (11)–(14) yields the approximate relationships

$$K_{yy}\simeq\overline{Vl}\equiv K \tag{20}$$

$$K_{yz}=K_{zy}\simeq\overline{Vl\alpha}=\bar{\alpha}K \tag{21}$$

$$K_{zz}\simeq\overline{Vl}(\bar{\alpha}^2+\overline{\alpha'^2})=(\bar{\alpha}^2+\overline{\alpha'^2})K \tag{22}$$

In obtaining (20)–(22) it has been necessary to assume that $\bar{\alpha}$ and $\overline{\alpha'^2}$ are independent of V (and l), that is, that the slope of the mixing path and its variance ($\overline{\alpha'^2}$) do not depend on the wind speed or the length of the path.

Upon substituting (20)–(22) in (9) and (10) and making use of the relationship

$$\bar{\beta}\simeq\tan\bar{\beta}=-\frac{\partial\bar{\chi}}{\partial y}\Big/\frac{\partial\bar{\chi}}{\partial z} \tag{23}$$

where $\bar{\beta}$ is the slope of the $\bar{\chi}$-surface, we obtain the alternative expressions for the fluxes

$$F_y=-\rho K\left(1-\frac{\bar{\alpha}}{\bar{\beta}}\right)\frac{\partial\bar{\chi}}{\partial y} \tag{24}$$

$$F_z=-\rho K(\bar{\alpha}^2+\overline{\alpha'^2}-\bar{\alpha}\bar{\beta})\frac{\partial\bar{\chi}}{\partial z} \tag{25}$$

which also may be written, with sufficient accuracy,

$$F_y=-\rho K_{yy}\left(1-\frac{\bar{\alpha}}{\bar{\beta}}\right)\frac{\partial\bar{\chi}}{\partial y} \tag{26}$$

$$F_z=-\rho K_{zz}\left(1-\frac{\bar{\alpha}\bar{\beta}}{\bar{\alpha}^2+\overline{\alpha'^2}}\right)\frac{\partial\bar{\chi}}{\partial z} \tag{27}$$

From (24) or (26) it is seen that the direction of the meridional flux is determined by whether $\bar{\alpha}$ (hereafter referred to as the slope of the preferred mixing surface) is greater or less than $\bar{\beta}$, the slope of the $\bar{\chi}$-surface. For $\bar{\alpha}>\bar{\beta}$, the case illustrated in figure 1, F_y and $\partial\bar{\chi}/\partial y$ have the same sign and the flux is countergradient. This is the condition which applies in the lower stratosphere with respect to the heat and ozone fluxes. In the extratropical troposphere it is known from baroclinic theory that the slope of the preferred mixing surface is about one-half the slope of the undisturbed isentropic surfaces ($\bar{\alpha}<\bar{\beta}$); thus the heat flux is in the direction of the gradient, as confirmed by measurement. For $\bar{\alpha}=0$, equation (26) reduces to the commonly used form shown in equation (6). It is apparent that this form is permissible only in those limited portions of the atmosphere where the large-scale exchange processes take place predominantly in the horizontal plane.

The direction of the vertical flux cannot be deduced so readily from the corresponding equations, (25) and (27). If $\bar{\beta}<\bar{\chi}$, F_z is of opposite sign to $\partial\bar{\chi}/\partial z$ and the flux is in the direction of the gradient. However, $\bar{\beta}$ must exceed $\bar{\alpha}$ by a finite margin, determined by the size of $\overline{\alpha'^2}$, before the vertical flux can become countergradient. As regards sensible heat or enthalpy there can be no question that vertical countergradient flux occurs in the troposphere. This is attested to by the fact that warm air rises and cold air sinks in the large-scale extratropical disturbances, producing an upward heat flux despite the upward increase of mean potential temperature.

6. PRACTICAL APPLICATION

When the expressions (9) and (10) for the eddy fluxes are substituted in (3), the diffusion equation becomes

$$\frac{\partial\bar{c}}{\partial t}=-\bar{\mathbf{V}}\cdot\nabla\bar{c}-\Gamma\overline{wc}+\frac{\partial}{\partial y}\left(\rho K_{yy}\frac{\partial\bar{\chi}}{\partial y}\right)+\frac{\partial}{\partial y}\left(\rho K_{yz}\frac{\partial\bar{\chi}}{\partial z}\right)+\frac{\partial}{\partial z}\left(\rho K_{yz}\frac{\partial\bar{\chi}}{\partial y}\right)+\frac{\partial}{\partial z}\left(\rho K_{zz}\frac{\partial\bar{\chi}}{\partial z}\right)-\frac{\rho\tan\phi}{a}\left(K_{yy}\frac{\partial\bar{\chi}}{\partial y}+K_{yz}\frac{\partial\bar{\chi}}{\partial z}\right) \tag{28}$$

or with further use of the relation $\bar{c}=\rho\bar{\chi}$

$$\frac{\partial\bar{c}}{\partial t}=-\bar{\mathbf{V}}\cdot\nabla\bar{c}-\Gamma\overline{wc}+\frac{\partial}{\partial y}\left(K_{yy}\frac{\partial\bar{c}}{\partial y}\right)+\frac{\partial}{\partial y}\left(K_{yz}\frac{\partial\bar{c}}{\partial z}\right)+\frac{\partial}{\partial z}\left(K_{yz}\frac{\partial\bar{c}}{\partial y}\right)+\frac{\partial}{\partial z}\left(K_{zz}\frac{\partial\bar{c}}{\partial z}\right)+\frac{\partial}{\partial z}\left(\Gamma K_{zz}\bar{c}\right)-\frac{\tan\phi}{a}\left(K_{yy}\frac{\partial\bar{c}}{\partial y}+K_{yz}\frac{\partial\bar{c}}{\partial z}+\Gamma K_{yz}\bar{c}\right) \tag{29}$$

For prescribed initial and boundary conditions, equation (29) may be solved numerically to give the time variation of the $\bar{c}$-distribution provided the values of K_{yy}, K_{yz}, K_{zz} (and other parameters) are known. We now consider the problem of evaluating these coefficients. An empirical approach which makes use of actual flux data appears required, and immediately the difficulty arises that there are three unknown coefficients and

TABLE 1.—*Eddy diffusion coefficients based on heat flux data: January–March*

	Latitude							
	10	20	30	40	50	60	70	80
	100 mb.							
K_{yy} (10^{10} cm.^{2} sec.$^{-1}$)	2.2	3.2	3.7	3.6	4.1	5.0	5.9	5.4
K_{yz} (10^8 cm.^{2} sec.$^{-1}$)	−8.4	−16.1	−31.5	−26.7	−22.5	−15.4	−4.9	−5.7
K_{zz} (10^3 cm.^{2} sec.$^{-1}$)	6.1	12.6	31.0	25.0	17.7	9.6	6.1	5.9
	50 mb.							
K_{yy} (10^{10} cm.^{2} sec.$^{-1}$)	.9	1.0	1.3	2.1	3.4	4.4	6.4	7.1
K_{yz} (10^8 cm.^{2} sec.$^{-1}$)	−1.2	−3.0	−7.1	−12.3	−17.9	−18.9	−22.0	−11.4
K_{zz} (10^3 cm.^{2} sec.$^{-1}$)	1.0	1.9	5.1	9.4	12.9	12.4	13.6	8.7
	30 mb.							
K_{yy} (10^{10} cm.^{2} sec.$^{-1}$)	.7	.8	1.2	2.2	4.6	5.3	6.0	6.1
K_{yz} (10^8 cm.^{2} sec.$^{-1}$)	−1.3	−1.7	−3.0	−5.6	−10.5	−15.3	−15.5	−8.4
K_{zz} (10^3 cm.^{2} sec.$^{-1}$)	1.0	1.2	2.0	2.6	6.9	9.6	9.9	7.2

TABLE 2.—*Eddy diffusion coefficients based on heat flux data: April–June*

	Latitude							
	10	20	30	40	50	60	70	80
	100 mb.							
K_{yy} (10^{10} cm.^{2} sec.$^{-1}$)	1.4	1.9	2.3	2.4	2.1	1.7	1.5	1.0
K_{yz} (10^8 cm.^{2} sec.$^{-1}$)	−4.8	−8.5	−16.9	−21.3	−15.1	−10.7	−4.3	.8
K_{zz} (10^3 cm.^{2} sec.$^{-1}$)	3.6	6.4	15.1	21.4	13.5	9.2	3.3	1.4
	50 mb.							
K_{yy} (10^{10} cm.^{2} sec.$^{-1}$)	.6	.5	.6	1.0	1.1	.9	1.0	.9
K_{yz} (10^8 cm.^{2} sec.$^{-1}$)	−.9	−1.1	−2.0	−4.8	−5.4	−5.7	−4.5	1.4
K_{zz} (10^3 cm.^{2} sec.$^{-1}$)	.9	.9	1.4	3.8	4.3	5.1	3.2	1.4
	30 mb.							
K_{yy} (10^{10} cm.^{2} sec.$^{-1}$)	.5	.4	.4	.7	.8	.9	1.0	.7
K_{yz} (10^8 cm.^{2} sec.$^{-1}$)	−.7	−.8	−.7	−1.3	−2.4	−5.0	−3.5	2.2
K_{zz} (10^3 cm.^{2} sec.$^{-1}$)	.8	.7	.6	1.2	1.8	3.7	2.5	1.6

only two equations available (for instance (9) and (10)). A way around this difficulty is the following.

We begin by assuming that in the baroclinically most active part of the atmosphere, the relation $\bar{\alpha}=\bar{\beta}/2$, derived first by Eady [4], holds, $\bar{\beta}$ being the slope of the isentropes. The middle troposphere at 50°N. is assumed to fulfill best this condition. Thus in this limited region, the meridional heat flux is given by

$$H_y=-\frac{\rho c_p K_{yy}}{2}\frac{\partial\bar{\theta}}{\partial y} \tag{30}$$

where c_p is the specific heat at constant pressure and θ is the potential temperature. With use of this equation heat flux and temperature data appearing in Peixoto [16] may be used to obtain K_{yy}.

We next make the common assumption that K_{yy} is proportional to the variance of the meridional wind component and use data presented by Buch [2], Murakami [12], and Peng [17] to scale K_{yy} to other levels and latitudes. Buch's data refer to transient eddies only, but rough estimates indicate that this limitation is of little practical importance. Heat flux and temperature data for these other areas (Oort [15]) are next substituted in (26) to yield the distribution of $\bar{\alpha}$. Values of K_{yz} may then be computed from equations (20) and (21).

With use of comparable data on vertical heat flux, equation (10) can be employed to solve finally for K_{zz}. However, since such data are of questionable reliability because of the inaccuracies of the vertical velocity measurements, we prefer to seek a different method. Equations (20) and (22) offer a possible method provided $\overline{\alpha'^2}$ can be estimated. To make such an estimate we note that by reason of symmetry $\bar{\alpha}=0$ at or near the equator. Thus in the equatorial zone

$$\overline{\alpha'^2}=\frac{K_{zz}}{K_{yy}} \tag{31}$$

From the rate of vertical spread of the tungsten-185 cloud, Spar [7] has estimated a value of 10^3 cm.^{2} sec.$^{-1}$ for K_{zz} in the lower stratosphere near the equator. This

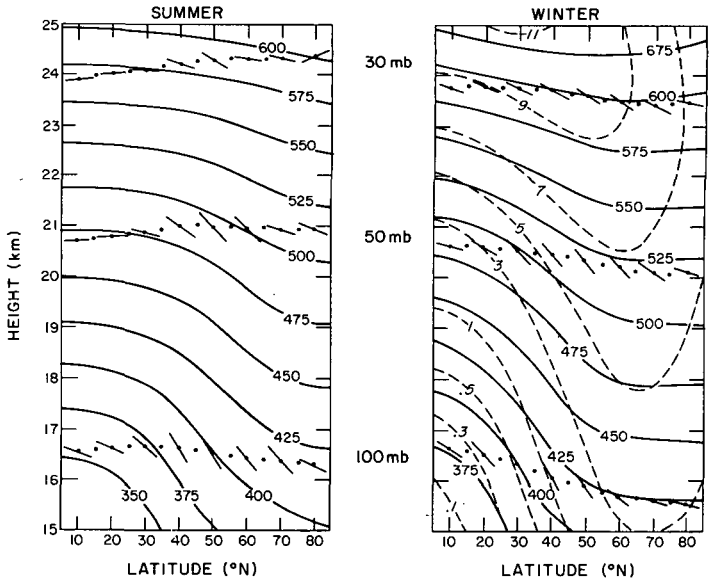

FIGURE 2.—Slopes of surfaces of preferred mixing (short line segments) for summer and winter seasons as derived from heat flux data. Solid lines represent mean potential temperature (°A.) and dashed lines mean ozone mixing ratio (μgm./gm.) after Newell [13].

figure with the appropriate scaled value of K_{yy} gives $\overline{\alpha'^2}$ at the equator. Equation (22) may now be employed to solve for K_{zz} at other latitudes and heights by use of the computed values of $\bar{\alpha}$ and $\overline{\alpha'^2}$. Not knowing how $\overline{\alpha'^2}$ varies with latitude and height, we assume that it remains constant.

Tables 1–4 give values of K_{yy}, K_{yz}, and K_{zz} computed in the foregoing manner for each of the four seasons. Supplementary data used in computing the coefficients appear in tables 5–9.

From the physical standpoint perhaps the most interesting result shown in the tables is the distribution of $\bar{\alpha}$. This is depicted graphically in figure 2 where the short line segments indicate the slope of the preferred mixing surfaces. Also shown on the diagram are the isentropic surfaces and, for the winter season only, the isopleths of

TABLE 3.—*Eddy diffusion coefficients based on heat flux data: July–September*

	Latitude							
	10	20	30	40	50	60	70	80
	100 mb.							
K_{yy} (10^{10} cm.^{2} sec.$^{-1}$)	1.5	2.0	2.7	2.6	2.1	1.2	0.7	0.6
K_{yz} (10^6 cm.^{2} sec.$^{-1}$)	−3.8	−5.8	−12.4	−22.2	−16.0	−7.0	−3.7	−1.7
K_{zz} (10^3 cm.^{2} sec.$^{-1}$)	2.9	4.3	9.3	22.2	14.9	6.1	3.2	1.2
	50 mb.							
K_{yy} (10^{10} cm.^{2} sec.$^{-1}$)	.7	.9	.9	.8	.6	.5	.4	.5
K_{yz} (10^6 cm.^{2} sec.$^{-1}$)	.02	−.5	−1.8	−3.8	−3.6	−2.8	−.5	−1.1
K_{zz} (10^3 cm.^{2} sec.$^{-1}$)	1.0	1.2	1.6	2.8	3.0	2.2	.6	.9
	30 mb.							
K_{yy} (10^{10} cm.^{2} sec.$^{-1}$)	.8	1.1	.9	.8	.6	.5	.4	.3
K_{yz} (10^6 cm.^{2} sec.$^{-1}$)	−.2	−.6	−1.3	−2.3	−2.4	−.4	−.5	.6
K_{zz} (10^3 cm.^{2} sec.$^{-1}$)	1.1	1.5	1.4	1.8	1.7	4.3	.6	.5

TABLE 4.—*Eddy diffusion coefficients based on heat flux data: October–December*

	Latitude							
	10	20	30	40	50	60	70	80
	100 mb.							
K_{yy} (10^{10} cm.^{2} sec.$^{-1}$)	2.5	3.5	4.6	4.6	4.1	4.2	2.9	2.1
K_{yz} (10^6 cm.^{2} sec.$^{-1}$)	−6.5	−11.4	−28.2	−35.0	−24.7	−16.0	8.6	18.2
K_{zz} (10^3 cm.^{2} sec.$^{-1}$)	5.1	8.2	23.7	32.7	20.7	11.6	6.3	18.1
	50 mb.							
K_{yy} (10^{10} cm.^{2} sec.$^{-1}$)	.9	1.2	1.6	1.9	2.7	3.8	4.0	1.7
K_{yz} (10^6 cm.^{2} sec.$^{-1}$)	−1.0	−2.2	−5.1	−9.2	−14.1	−6.7	14.6	11.6
K_{zz} (10^3 cm.^{2} sec.$^{-1}$)	1.3	2.0	3.7	7.0	11.1	6.2	10.6	10.4
	30 mb.							
K_{yy} (10^{10} cm.^{2} sec.$^{-1}$)	1.0	.9	1.1	1.6	2.7	4.6	5.2	2.1
K_{yz} (10^6 cm.^{2} sec.$^{-1}$)	−1.1	−.7	.1	−.4	−4.9	−2.7	16.2	8.0
K_{zz} (10^3 cm.^{2} sec.$^{-1}$)	1.4	1.3	1.5	2.2	4.5	6.3	11.9	6.0

TABLE 5.—*Estimated values of K_{yy} at 50° N. in the middle troposphere and in the lower stratosphere (100 mb.). Temperature data are from Peixoto [16]; wind variances from Buch [2].*

	Summer	Winter
$\overline{v'\theta'}$ (deg. cm. sec.$^{-1}$)	7.43×10^{2}	16.61×10^{2}
$\partial\bar{\theta}/\partial y$ (deg. cm.$^{-1}$)	-5.1×10^{-8}	-6.5×10^{-8}
K_{yy} (trop.) (cm.^{2} sec.$^{-1}$)	2.9×10^{10}	5.1×10^{10}
$\sigma^2(v)$ (trop.) (m.^{2} sec.$^{-2}$)	88.4	121.0
$\sigma^2(v)$ (100 mb.) (m.^{2} sec.$^{-2}$)	64.0	96.0
K_{yy} (100 mb.) (cm.^{2} sec.$^{-1}$)	2.1×10^{10}	4.1×10^{10}

TABLE 6.—*Supplementary data used in computing eddy diffusion coefficients: January–March*

	Latitude							
	10	20	30	40	50	60	70	80
	100 mb.							
$\overline{v'\theta'}$ (10^3 deg. cm. sec.$^{-1}$)	0.52	0.21	0.47	1.05	3.01	3.72	1.13	0.13
$\sigma^2(v)$ (10^5 cm.^{2} sec.$^{-2}$)	4.44	6.25	7.40	7.03	8.01	9.84	11.66	10.65
$\bar{\theta}$ (deg. A.)	377	385	401	416	424	423	423	423
$\partial\bar{\theta}/\partial y$ (10^{-8} deg. cm.$^{-1}$)	6.3	10.4	15.1	10.9	3.0	−1.6	−.3	1.7
$\partial\bar{\theta}/\partial z$ (10^{-4} deg. cm.$^{-1}$)	2.3	2.2	2.0	1.9	1.9	1.9	1.9	1.9
$\bar{\beta}$ (10^{-4})	−2.7	−4.8	−7.8	−5.9	−1.6	.8	.2	−.9
$\bar{\alpha}$ (10^{-4})	−3.8	−5.1	−8.4	−7.5	−5.5	−3.1	−.8	−1.1
	50 mb.							
$\overline{v'\theta'}$ (10^3 deg. cm. sec.$^{-1}$)	−.08	.13	.62	1.33	3.30	5.06	5.22	1.32
$\sigma^2(v)$ (10^5 cm.^{2} sec.$^{-2}$)	1.76	1.99	2.63	4.09	6.72	8.61	12.70	13.98
$\bar{\theta}$ (deg. A.)	483	489	499	511	517	517	515	516
$\partial\bar{\theta}/\partial y$ (10^{-8} deg. cm.$^{-1}$)	5.1	7.6	10.0	8.3	2.5	−1.7	−.4	1.7
$\partial\bar{\theta}/\partial z$ (10^{-4} deg. cm.$^{-1}$)	3.0	3.0	2.7	2.5	2.3	2.3	2.3	2.2
$\bar{\beta}$ (10^{-4})	−1.7	−2.6	−3.7	−3.3	−1.1	.7	.2	−.8
$\bar{\alpha}$ (10^{-4})	−1.4	−3.0	−5.4	−5.9	−5.3	−4.3	−3.4	−1.6
	30 mb.							
$\overline{v'\theta'}$ (10^3 deg. cm. sec.$^{-1}$)	.11	.29	.62	1.44	3.56	4.95	4.53	2.98
$\sigma^2(v)$ (10^5 cm.^{2} sec.$^{-2}$)	1.31	1.56	2.31	4.35	8.99	10.43	11.86	12.12
$\bar{\theta}$ (deg. A.)	587	593	597	599	599	597	594	594
$\partial\bar{\theta}/\partial y$ (10^{-8} deg. cm.$^{-1}$)	5.4	4.2	3.2	1.0	−1.7	−2.0	−1.0	−1.5
$\partial\bar{\theta}/\partial z$ (10^{-4} deg. cm.$^{-1}$)	3.6	3.6	3.3	2.9	2.7	2.6	2.5	2.5
$\bar{\beta}$ (10^{-4})	−1.5	−1.2	−1.0	−.3	.6	.8	.4	.6
$\bar{\alpha}$ (10^{-4})	−2.0	−2.2	−2.6	−2.6	−2.3	−2.9	−2.6	−1.4

ozone mixing ratio. In general the mixing surfaces incline downward from equator to pole. Greatest inclinations occur in middle latitudes and at lower levels. The slopes are nearly everywhere greater than the slopes of the undisturbed isentropes and nearly the same as, or slightly less than, the slopes of the ozone mixing ratio lines. Evidently the slopes of the mixing surfaces determined from the heat flux data are too small to account for the countergradient flux of ozone. This discrepancy may be due to inaccuracies in the data, but more likely stems from the fact that, because of radiative influences, potential temperature cannot be expected to behave as conservatively as ozone in the lower stratosphere. It can be shown by simple arguments that the effect of radiation is to cause the slopes of the mixing surfaces to be underestimated. Until numerical experiments are carried out using the coefficients given in tables 1–4, it is impossible to say how serious the apparent underestimate of the slopes may be,

TABLE 7.—*Supplementary data used in computing eddy diffusion coefficients: April–June*

	Latitude							
	10	20	30	40	50	60	70	80
	100 mb.							
$\overline{v'\theta'}$ (10^3 deg. cm. sec.$^{-1}$)	0.48	0.55	0.74	0.88	1.15	1.09	0.37	0.08
$\sigma^2(v)$ (10^5 cm.^{2} sec.$^{-2}$)	2.97	4.11	5.10	5.33	4.62	3.67	3.24	2.14
$\bar{\theta}$ (deg. A.)	378	385	398	415	427	433	438	439
$\partial\bar{\theta}/\partial y$ (10^{-8} deg. cm.$^{-1}$)	5.4	8.3	13.6	14.1	7.6	5.2	2.8	.7
$\partial\bar{\theta}/\partial z$ (10^{-4} deg. cm.$^{-1}$)	2.6	2.5	2.3	2.0	1.8	1.8	1.8	1.8
$\bar{\beta}$ (10^{-4})	−2.1	−3.3	−5.9	−6.9	−4.2	−2.8	−1.5	−.4
$\bar{\alpha}$ (10^{-4})	−3.5	−4.5	−7.2	−8.7	−7.1	−6.4	−2.9	−.8
	50 mb.							
$\overline{v'\theta'}$ (10^3 deg. cm. sec.$^{-1}$)	−.01	−.01	.12	.44	.75	.88	.69	−.29
$\sigma^2(v)$ (10^5 cm.^{2} sec.$^{-2}$)	1.25	1.13	1.35	2.11	2.30	1.90	2.30	2.00
$\bar{\theta}$ (deg. A.)	491	497	505	514	521	527	532	533
$\partial\bar{\theta}/\partial y$ (10^{-8} deg. cm.$^{-1}$)	4.9	6.6	7.2	8.1	5.1	5.1	3.2	−.4
$\partial\bar{\theta}/\partial z$ (10^{-4} deg. cm.$^{-1}$)	3.1	3.0	2.8	2.6	2.4	2.3	2.3	2.3
$\bar{\beta}$ (10^{-4})	−1.6	−2.2	−2.6	−3.2	−2.1	−2.2	−1.4	.2
$\bar{\alpha}$ (10^{-4})	−1.5	−2.1	−3.2	−4.9	−5.1	−6.6	−4.3	1.6
	30 mb.							
$\overline{v'\theta'}$ (10^3 deg. cm. sec.$^{-1}$)	−.05	.13	.16	.30	.50	.88	.54	−.50
$\sigma^2(v)$ (10^5 cm.^{2} sec.$^{-2}$)	1.20	.98	.98	1.51	1.75	2.06	2.25	1.59
$\bar{\theta}$ (deg. A.)	596	601	604	605	607	611	616	618
$\partial\bar{\theta}/\partial y$ (10^{-8} deg. cm.$^{-1}$)	5.4	3.4	1.5	1.2	2.2	4.7	3.7	−1.0
$\partial\bar{\theta}/\partial z$ (10^{-4} deg. cm.$^{-1}$)	3.5	3.4	3.2	2.9	2.8	2.7	2.6	2.6
$\bar{\beta}$ (10^{-4})	−1.6	−1.0	−.5	−.4	−.8	−1.7	−1.4	.4
$\bar{\alpha}$ (10^{-4})	−1.3	−1.8	−1.5	−1.9	−3.0	−5.2	−3.4	3.0

TABLE 8.—*Supplementary data used in computing eddy diffusion coefficients; July–September*

	Latitude							
	10	20	30	40	50	60	70	80
	100 mb.							
$\overline{v'\theta'}$ (10^3 deg. cm. sec.$^{-1}$)	0.31	0.48	0.27	0.61	0.80	0.66	0.40	0.14
$\sigma^2(v)$ (10^5 cm.^{2} sec.$^{-2}$)	2.45	3.29	4.41	4.22	3.43	1.87	1.07	1.02
$\bar{\theta}$ (deg. A.)	381	386	394	410	425	433	437	442
$\partial\bar{\theta}/\partial y$ (10^{-8} deg. cm.$^{-1}$)	4.7	5.0	10.1	15.8	10.1	5.4	4.5	2.6
$\partial\bar{\theta}/\partial z$ (10^{-4} deg. cm.$^{-1}$)	2.7	2.6	2.4	2.1	1.8	1.8	1.9	1.8
$\bar{\beta}$ (10^{-4})	−1.8	−2.0	−4.2	−7.4	−5.5	−2.9	−2.4	−1.4
$\bar{\alpha}$ (10^{-4})	−2.5	−2.9	−4.6	−8.5	−7.6	−6.1	−5.7	−2.6
	50 mb.							
$\overline{v'\theta'}$ (10^3 deg. cm. sec.$^{-1}$)	−.10	−.14	.02	.33	.49	.39	−.07	.05
$\sigma^2(v)$ (10^5 cm.^{2} sec.$^{-2}$)	1.21	1.49	1.42	1.30	.94	.79	.63	.77
$\bar{\theta}$ (deg. A.)	498	500	505	513	522	528	534	539
$\partial\bar{\theta}/\partial y$ (10^{-8} deg. cm.$^{-1}$)	1.3	3.0	5.7	8.5	6.8	5.3	4.9	4.2
$\partial\bar{\theta}/\partial z$ (10^{-4} deg. cm.$^{-1}$)	3.0	2.9	2.8	2.7	2.5	2.4	2.4	2.3
$\bar{\beta}$ (10^{-4})	−.4	−1.0	−2.0	−3.2	−2.7	−2.2	−2.1	−1.8
$\bar{\alpha}$ (10^{-4})	0.3	−.5	−2.1	−4.8	−6.2	−5.6	−1.3	−2.2
	30 mb.							
$\overline{v'\theta'}$ (10^3 deg. cm. sec.$^{-1}$)	.07	.03	.05	.41	.50	−.06	−.06	−.26
$\sigma^2(v)$ (10^5 cm.^{2} sec.$^{-2}$)	1.37	1.73	1.46	1.25	1.05	.77	.60	.43
$\bar{\theta}$ (deg. A.)	599	600	602	607	611	615	620	626
$\partial\bar{\theta}/\partial y$ (10^{-8} deg. cm.$^{-1}$)	(10^{-5})	1.5	3.9	3.9	3.4	3.7	5.4	3.9
$\partial\bar{\theta}/\partial z$ (10^{-4} deg. cm.$^{-1}$)	3.2	3.2	3.2	3.1	2.9	2.8	2.7	2.69
$\bar{\beta}$ (10^{-4})	−(10^{-5})	−.5	−1.2	−1.3	−1.2	−1.3	−2.0	−1.5
$\bar{\alpha}$ (10^{-4})	−.3	−.5	−1.4	−3.0	−3.8	−.9	−1.4	2.1

TABLE 9.—*Supplementary data used in computing eddy diffusion coefficients: October–December*

	Latitude							
	10	20	30	40	50	60	70	80
	100 mb.							
$\overline{v'\theta'}$ (10^3 deg. cm. sec.$^{-1}$)	0.26	0.10	0.46	1.22	2.37	2.65	0.12	−1.19
$\sigma^2(v)$ (10^5 cm.^{2} sec.$^{-2}$)	3.10	4.44	5.71	5.76	5.07	5.29	3.68	2.67
$\bar{\theta}$ (deg. A.)	377	384	395	410	419	422	419	412
$\partial\bar{\theta}/\partial y$ (10^{-8} deg. cm.$^{-1}$)	5.7	7.3	12.3	12.2	5.3	.3	−5.2	−7.6
$\partial\bar{\theta}/\partial z$ (10^{-4} deg. cm.$^{-1}$)	2.6	2.4	2.2	2.0	1.8	1.7	1.6	1.5
$\bar{\beta}$ (10^{-4})	−2.2	−3.1	−5.7	−6.2	−2.9	−.2	3.2	4.9
$\bar{\alpha}$ (10^{-4})	−2.6	−3.2	−6.2	−7.6	−6.1	−3.8	2.9	8.5
	50 mb.							
$\overline{v'\theta'}$ (10^3 deg. cm. sec.$^{-1}$)	.03	.22	.55	1.37	2.84	2.65	.06	−1.11
$\sigma^2(v)$ (10^5 cm.^{2} sec.$^{-2}$)	1.11	1.44	2.02	2.38	3.36	4.72	5.00	2.07
$\bar{\theta}$ (deg. A.)	491	495	500	507	511	510	504	494
$\partial\bar{\theta}/\partial y$ (10^{-8} deg. cm.$^{-1}$)	3.2	3.9	5.5	5.1	1.6	−3.1	−8.2	−8.7
$\partial\bar{\theta}/\partial z$ (10^{-4} deg. cm.$^{-1}$)	3.1	3.0	2.8	2.5	2.3	2.2	2.2	2.2
$\bar{\beta}$ (10^{-4})	−1.0	−1.3	−1.9	−2.0	−.7	1.4	3.7	3.9
$\bar{\alpha}$ (10^{-4})	−1.1	−1.9	−3.2	−4.8	−5.3	−1.8	3.7	7.0
	30 mb.							
$\overline{v'\theta'}$ (10^3 deg. cm. sec.$^{-1}$)	−.01	.12	.17	.84	2.15	2.62	.34	−.83
$\sigma^2(v)$ (10^5 cm.^{2} sec.$^{-2}$)	1.26	1.17	1.40	2.02	3.39	5.70	6.55	2.57
$\bar{\theta}$ (deg. A.)	597	601	600	597	592	589	581	572
$\partial\bar{\theta}/\partial y$ (10^{-8} deg. cm.$^{-1}$)	3.9	1.5	−2.0	−4.4	−3.1	−4.2	−8.7	−6.4
$\partial\bar{\theta}/\partial z$ (10^{-4} deg. cm.$^{-1}$)	3.5	3.6	3.4	3.0	2.7	2.6	2.6	2.7
$\bar{\beta}$ (10^{-4})	−1.1	−.4	.6	1.5	1.1	1.6	3.3	2.4
$\bar{\alpha}$ (10^{-4})	−1.1	−.8	.1	−.3	−1.8	−.6	3.1	3.9

but results of the next section suggest that it is not crucial.

7. A CRUDE ANALYTICAL SOLUTION USING THE TUNGSTEN-185 DATA

Though it is not our intent at this time to present numerical solutions to equation (29), it is interesting to attempt a simple analytical solution which will give at least a crude idea of the usefulness of the concepts developed in the previous sections. To achieve such a solution we will neglect the terms involving mean motions and the spherical shape of the earth and will assume that Γ and the eddy diffusion coefficients are constant. Finally we will rotate the coordinate axes into the principal axis system thereby eliminating the terms in K_{yz}. The rotation to a principal axis system is possible because of our earlier assumption that the diffusion matrix is symmetrical ($K_{yz}=K_{zy}$). When the foregoing steps are taken (29) assumes the simple form

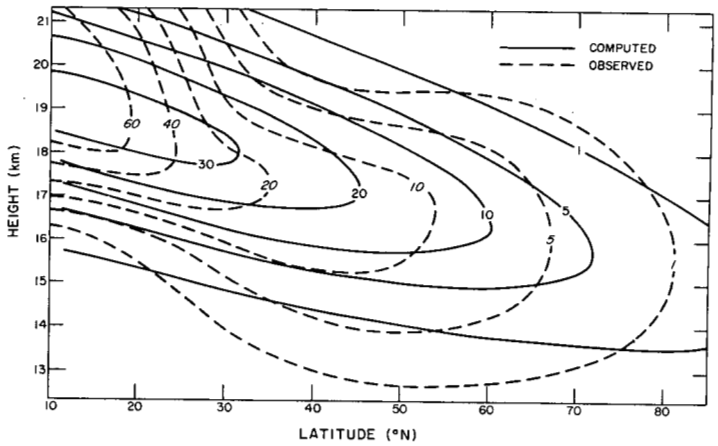

FIGURE 3.—Predicted and observed distributions of tungsten-185 two months after time of injection assumed to be August 1, 1958. Units: d.p.m./1000 SCF.

$$\frac{\partial\bar{c}}{\partial t}=K_Y\frac{\partial^2\bar{c}}{\partial Y^2}+K_Z\frac{\partial^2\bar{c}}{\partial Z^2}+\Gamma K_Z\frac{\partial\bar{c}}{\partial Z} \tag{32}$$

where Y, Z denote the rotated coordinate axes and K_Y, K_Z, are the eddy diffusion coefficients in the rotated system.

The required angle of rotation and the values of the coefficients may be obtained as follows. In matrix notation equations (9) and (10) are written

$$-\rho\begin{pmatrix}K_{yy} & K_{yz}\\ K_{yz} & K_{zz}\end{pmatrix}\begin{pmatrix}\partial\bar{\chi}/\partial y\\ \partial\bar{\chi}/\partial z\end{pmatrix}=\begin{pmatrix}F_y\\ F_z\end{pmatrix} \tag{33}$$

If the diffusion matrix in the original coordinate system (P) is denoted by M^P and in the rotated system (Q) by M^Q then we may transform the matrix from one system to the other by the relation (Rojansky [19])

$$M^Q=SM^PS^{-1} \tag{34}$$

where

$$S=\begin{pmatrix}\cos\gamma & \sin\gamma\\ -\sin\gamma & \cos\gamma\end{pmatrix},\quad S^{-1}=\begin{pmatrix}\cos\gamma & -\sin\gamma\\ \sin\gamma & \cos\gamma\end{pmatrix} \tag{35}$$

γ being the angle of rotation.

Thus carrying out the matrix multiplication, we find that

$$S\begin{pmatrix}K_{yy} & K_{yz}\\ K_{yz} & K_{zz}\end{pmatrix}S^{-1}=\begin{pmatrix}K_{yy}\cos^2\gamma+K_{yz}\sin 2\gamma+K_{zz}\sin^2\gamma & -\frac{K_{yy}}{2}\sin 2\gamma+K_{yz}\cos 2\gamma+\frac{K_{zz}}{2}\sin 2\gamma\\ -\frac{K_{yy}}{2}\sin 2\gamma+K_{yz}\cos 2\gamma+\frac{K_{zz}\sin 2\gamma}{2} & K_{yy}\sin^2\gamma-K_{yz}\sin 2\gamma+K_{zz}\cos^2\gamma\end{pmatrix} \tag{36}$$

In the principal axis system the off-diagonal terms are zero. Hence

$$\frac{K_{zz}-K_{yy}}{2}\sin 2\gamma+K_{yz}\cos 2\gamma=0 \tag{37}$$

or

$$\tan 2\gamma=\frac{2K_{yz}}{K_{yy}-K_{zz}} \tag{38}$$

Substitution of equations (20)–(22) gives

$$\tan 2\gamma=\frac{2\bar{\alpha}}{1-\bar{\alpha}^2-\overline{\alpha'^2}}\simeq 2\bar{\alpha} \tag{39}$$

Since α is a small angle, it follows that

$$\gamma=\bar{\alpha} \tag{40}$$

and therefore that for all practical purposes the inclination of the principal axis and the slope of the preferred mixing surface are identical.

Again using the relationships (20)–(22) in the diagonal terms and neglecting higher order effects, we obtain for the flux in the principal axis system

$$-\rho\begin{pmatrix}K_{yy} & 0\\ 0 & \overline{\alpha'^2}K_{yy}\end{pmatrix}\begin{pmatrix}\partial\bar{x}/\partial Y\\ \partial\bar{x}/\partial Z\end{pmatrix}=\begin{pmatrix}F_Y\\ F_z\end{pmatrix} \tag{41}$$

Thus

$$K_Y=K_{yy}$$

$$K_Z=\overline{\alpha'^2}K_{yy} \tag{42}$$

Jost [9] gives the following solution to (32) for diffusion from an instantaneous point source.

$$\bar{c}=\frac{Q}{4\pi t(K_YK_Z)^{1/2}}\exp\left[-\frac{1}{4t}\left(\frac{Y^2}{K_Y}+\frac{Z^2}{K_Z}\right)-\frac{\Gamma Z}{2}-\frac{\Gamma^2K_Zt}{4}\right] \tag{43}$$

where Q is the strength of the source. By regarding the injection of tungsten-185 into the lower equatorial stratosphere during the Hardtack test series as an instantaneous point source, it is possible to solve (32) for an actual case. Since the tungsten-185 was introduced in several bursts over a small but finite height range and a period of two to three months, this is admittedly a crude assumption. In carrying out our solution we have assumed a mean value of K_{yy} from table 4 of 1.2×10^{10} cm.^{2} sec.$^{-1}$, and a value, as obtained from (31), of 1.1×10^{-7} for $\overline{\alpha'^2}$, giving a K_Z of 1.4×10^3 cm.^{2} sec.$^{-1}$ For the inclination of the principal axis we have taken a representative value of $\bar{\alpha}$ from table 9 of 5×10^{-4}. The initial amount of tungsten-185 was assumed to be 58 megacuries in accordance with the figure given in [7]. This amount was divided by the circumference of the earth in centimeters to give the source per unit distance of longitude. Thus we have assumed in effect that the mixing about the latitude circle was complete, uniform, and instantaneous. The latitude of injection was taken as 11°N. and the height as 19 km. The latter figure is about 1 km. less than the height estimated in [7] for the center of the cloud and was purposely chosen to give the best agreement between observed and computed distributions. We justify this procedure by noting that our main object here is to demonstrate the *shape* of the pattern established by the diffusion rather than the exact position of its center and by noting too that there is some uncertainty concerning the level of injection.

The solution two months after the time of injection (assumed to be August 1, 1958) is shown in figure 3. Only the pattern north of the latitude of injection is of interest because it is only here that the principal axis has been aligned with the mean slope of the mixing surface. Also shown in the figure is the observed distribution based on a gross smoothing of data given in [7].

There is sufficient agreement between computed and observed patterns to suggest that the inclined mixing process deduced here from the heat flux data may in itself account for the main features of the distribution. Minor discrepancies are evident. For instance, predicted amounts are too small at the higher levels near the latitude of injection and are too large at extratropical latitudes in the vicinity of the principal axis; but to what extent these disagreements are caused by the neglect of advective motions and to what extent they reflect the crudity of the assumptions (point source, constant diffusion coefficients, etc.) is difficult to ascertain without carrying out the more precise numerical calculations. Thus, a critical discussion of the error sources does not appear warranted at this time.

8. SUMMARY AND CONCLUSIONS

The usual Fickian formulation of the large-scale mixing problem is not valid in the lower stratosphere since it is unable to account for the observed (horizontal) countergradient flux of sensible heat and ozone. On the basis of the mixing length hypothesis we have shown that the Fickian law applies only when the exchange paths are horizontal on the average. When the paths are inclined, additional diffusion coefficients, which depend essentially on the covariance of the vertical and meridional velocity components, appear in the flux equations.

By use of published data on eddy heat transport we have attempted to evaluate the various coefficients needed for a correct description of the large-scale mixing process. As a by-product of our computations estimates of the mean slopes of the mixing paths (slopes of the preferred mixing surfaces) have been obtained for the Northern Hemisphere at the 100-, 50-, and 30-mb. levels. In general the mixing is inclined downward from equator to pole, as inferred by Feely and Spar [5] from the spread of the tungsten-185. The inclination is greater than that of the mean isentropes and approximately the same as that of the isopleths of ozone mixing ratio.

By rotating the coordinates into the principal axis system, and with the help of simplifying assumptions, we have been able to obtain an analytical solution to the diffusion equation for the case of an instantaneous point source. Application of the solution to tungsten-185 data reveals broad agreement between computed and observed distributions two months after the time of injection. The computation, though crude, would seem to

support the claim of Feely and Spar that an inclined, large-scale mixing was the dominant process in determining the spread of the tungsten-185.

Because of the simplifying assumptions that were required in obtaining an analytical solution, it has not been possible to isolate likely causes of certain discrepancies which were noted between the predicted and observed distributions. A critical discussion of the accuracy of the mixing model must wait more exact numerical solutions which avoid these assumptions. A numerical experiment is now being designed in which the diffusion coefficients derived from the heat flux data will be applied to the tungsten-185 problem. It is anticipated that the gross features of the tungsten-185 distribution that will emerge from the numerical computations will not differ markedly from the features obtained in the approximate analytical solution.

ACKNOWLEDGMENT

The authors wish to thank Joshua Z. Holland for reading the manuscript and offering helpful criticisms.

REFERENCES

1. A. W. Brewer, "Evidence for a World Circulation Provided by Measurement of Helium and Water Vapor Distribution in the Stratosphere," *Quarterly Journal of the Royal Meteorological Society*, vol. 75, No. 326, Oct. 1949, pp. 351–363.
2. H. S. Buch, "Hemispheric Wind Conditions During the Year 1950," *Final Report*, Part 2, Contract No. AF 19–122–153, Massachusetts Institute of Technology, 1954.
3. G. M. B. Dobson, "Origin and Distribution of the Polyatomic Molecules in the Atmosphere," *Proceedings of the Royal Society*, Ser. A, vol. 236, No. 1205, 1956, pp. 187–192.
4. E. T. Eady, "Long Waves and Cyclone Waves," *Tellus*, vol. 1, No. 3, Aug. 1949, pp. 33–52.
5. H. W. Feely and J. Spar, "Tungsten-185 from Nuclear Bomb Tests as a Tracer for Stratospheric Meteorology," *Nature*, vol. 188, No. 4756, Dec. 1960, pp. 1062–1064.
6. J. P. Friend and H. W. Feely, *Fifth Quarterly Report*, Contract DA–49–146–X2–079 (DASA 1305), Isotopes, Inc., 1962.
7. J. P. Friend (Ed.), H. W. Feely, P. W. Krey, J. Spar, and A. Walton, "Discussion of Hasp Results," vol. 3 (DASA 1300), Defense Atomic Support Agency, Washington, D.C., Aug. 1961, 307 pp.
8. W. S. Hering and T. R. Borden, Jr., "An Analysis of the Seasonal and Synoptic-Scale Variations in the Vertical Ozone Distribution," International Atmospheric Ozone Symposium, Albuquerque, N. Mex., Sept. 1964.
9. W. Jost, *Diffusion in Solids, Liquids, and Gases*, Academic Press, 1952, 558 pp. (p. 47).
10. L. Machta and R. J. List, "Stratospheric Radioactivity Measurements," American Meteorological Society Conference on Stratospheric Meteorology, Minneapolis, Minn., Sept. 1959.
11. A. C. Molla, Jr. and C. J. Loisel, "On the Hemispheric Correlations of Vertical and Meridional Wind Components," *Geofisica Pura e Applicata*, vol. 51, No. 1, 1962, pp. 166–170.
12. T. Murakami, "Stratospheric Wind, Temperature, and Isobaric Height Conditions During the IGY Period—Part I," *Report No. 5*, Contract No. AT (30–1) 2241, Massachusetts Institute of Technology, 1962.
13. R. E. Newell, "The Circulation of the Upper Atmosphere," *Scientific American*, vol. 210, No. 3, Mar. 1964, pp. 62–74.
14. R. E. Newell, "The Transport of Trace Substances in the Atmosphere and Their Implications for the General Circulation of the Stratosphere," *Geofisica Pura e Applicata*, vol. 49, 1961, pp. 137–158.
15. A. H. Oort, "On the Energy Cycle in the Lower Stratosphere," *Report No. 9*, Contract No. AT (30–1) 2241, Massachusetts Institute of Technology, 1963.
16. J. P. Peixoto, "Hemispheric Temperature Conditions During the Year 1950," *Scientific Report No. 4*, Contract No. AF 19(604)–6108, Massachusetts Institute of Technology, 1960.
17. L. Peng, "Stratospheric Wind, Temperature, and Isobaric Height Conditions During the IGY Period—Part II," *Report No. 10*, Contract AT (30–1) 2241, Massachusetts Institute of Technology, 1963.
18. C. Prabhakara, "Effects of Non-Photochemical Processes on the Meridional Distribution and Total Amount of Ozone in the Atmosphere," *Monthly Weather Review*, vol. 91, No. 9, Sept, 1963, pp. 411–431.
19. V. Rojansky, *Introductory Quantum Mechanics*, Prentice-Hall, Inc., New York, 1938, 544 pp. (p. 362).
20. A. Sundström, "Stratospheric Transports as Deduced from Tracers," FOA 4 Rapport A4379–4551, Försvarets Forskningsanstalt Avdelning 4, Stockholm, June 1964.
21. R. M. White, "The Counter-Gradient Flux of Sensible Heat in the Lower Stratosphere," *Tellus*, vol. 6, No. 2, May 1954, pp. 177–179.
22. O. R. Wulf, "The Distribution of Atmospheric Ozone," *Proceedings, Eighth American Scientific Congress*, vol. 7, 1942, pp. 439–446.

[*Received November 27, 1964; revised December 31, 1964*]